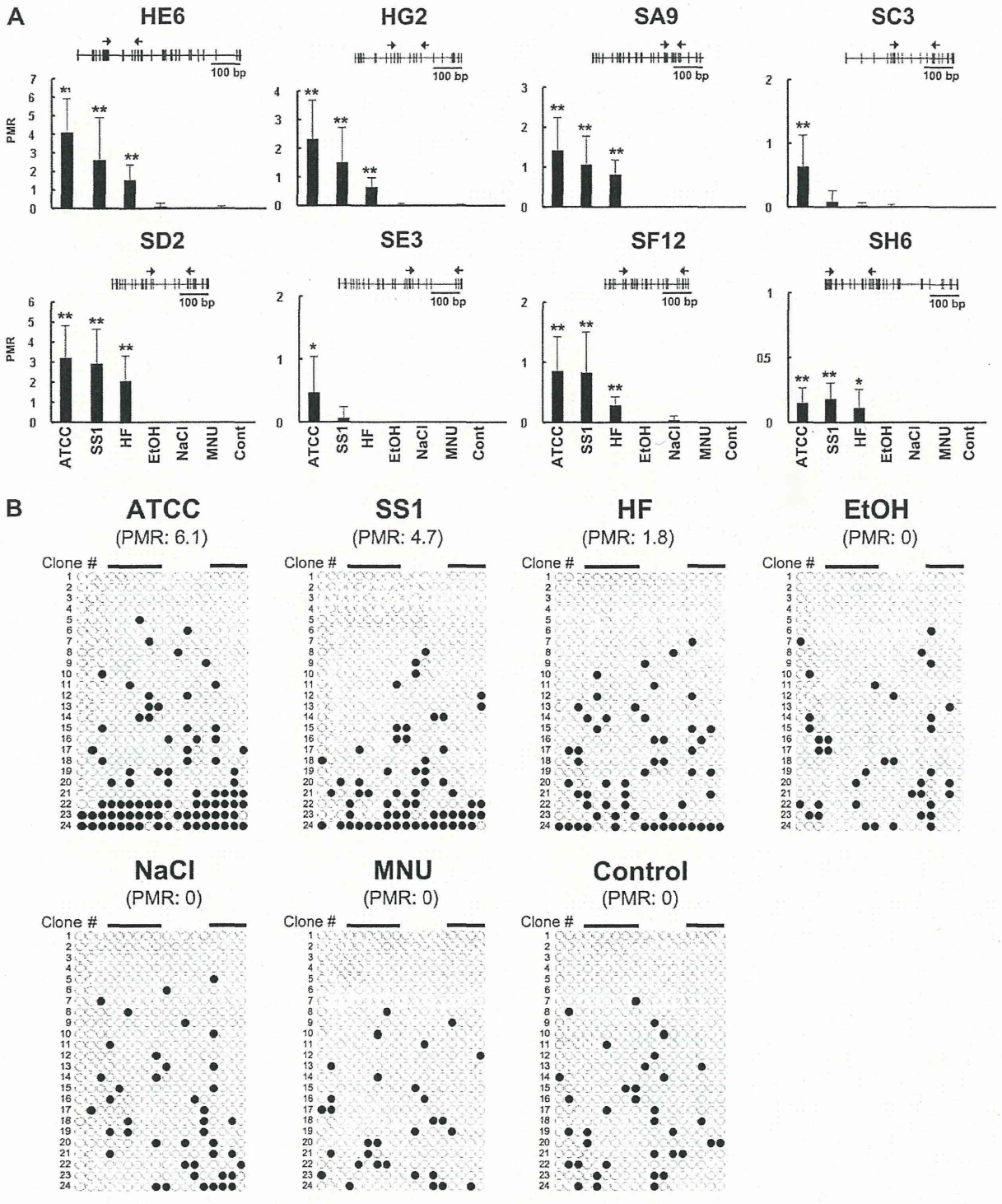

Fig. 2. Methylation induction in GECs by the three *Helicobacter*-induced inflammation but not by EtOH- or NaCl-induced inflammation. (**A**) Methylation levels of eight CGIs assessed by quantitative methylation-specific PCR. Upper panels show CpG maps, and lower panels show methylation levels in percentage of methylated reference. In the upper panel, vertical lines and arrows show individual CpG sites and positions of methylation-specific PCR primers, respectively. Values are shown as mean + SD. $^{*}P < 0.05$ and $^{**}P < 0.01$ compared with the control group. (**B**) Bisulfite sequencing of HE6 in GECs. Numbers in parentheses indicate percentage of methylated reference of the sample assessed by quantitative methylation-specific PCR. Bars, CpG sites on quantitative methylation-specific PCR primers.

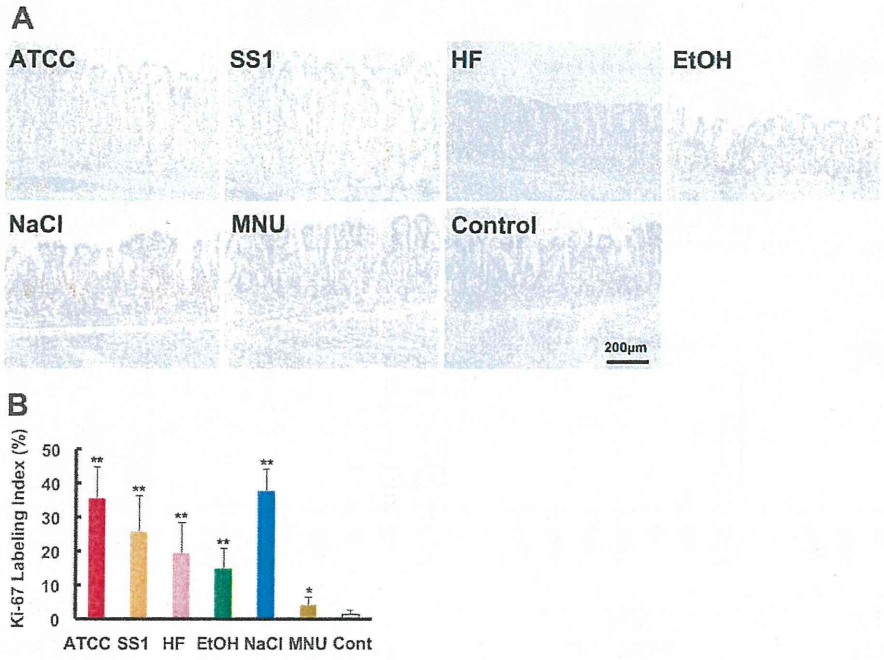

Fig. 3. Cell proliferation of gerbil GECs after the treatment. (**A**) Representative microscopic appearance of Ki-67 immunohistochemistry. (**B**) Ki-67 labeling index. Values are shown as mean + SD. $^{*}P < 0.05$ and $^{**}P < 0.01$ compared with the control group. The NaCl group showed a marked increase of cell proliferation.

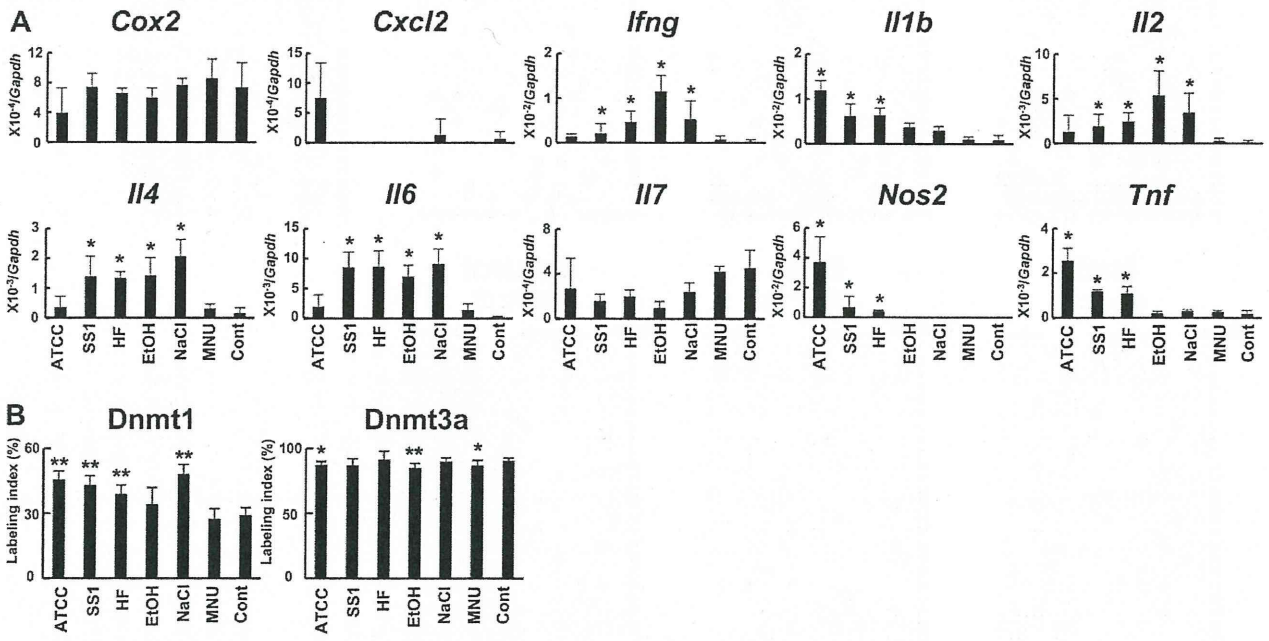

Fig. 4. Expression of inflammation-related genes and Dnmts in the gerbil stomach. (**A**) messenger RNA levels of inflammation-related genes in gerbil gastric tissues containing both mucosal and submucosal layers. Expression levels of *Il1b*, *Nos2* and *Tnf* were elevated only in the three *Helicobacter* groups. (**B**) The fractions of GECs expressing Dnmt proteins in gastric glands by immunohistochemistry. Values are shown as mean + SD. $^{*}P < 0.05$ and $^{**}P < 0.01$ compared with control group.

Human relevance of inflammation-related gene expression

To address whether upregulation of specific inflammation-related genes are common in the human stomach, we conducted qRT–PCR of *COX2*, *IFNG*, *IL1B*, *IL6*, *NOS2* and *TNF* using human gastric mucosa samples with and without *H.pylori* infection. Expression levels of *NOS2* and *TNF* were markedly upregulated (27- and 3-fold,

respectively) also in human gastric mucosae (Figure 5). However, *IL1B* expression tended to be lower in gastric mucosae of *H.pylori*-infected individuals.

Discussion

Among the five groups with inflammation, aberrant methylation was induced only in the three *Helicobacter* groups, which showed inflammation with infiltration of mononuclear cells, increased expression of *Il1b*, *Nos2* and *Tnf* and increased cell proliferation. In the EtOH and NaCl groups, these agents were administered repeatedly for 20 weeks, and increased cell proliferation was present at the end of the experiment. The increased proliferation was considered to have persisted for this period because thickening of lamina propria was observed in these two groups. Nevertheless, aberrant methylation was not induced, at least in the CGIs analyzed here. This showed that cell proliferation alone is not sufficient for methylation induction and suggested that both specific types of inflammation and increased cell proliferation are necessary for induction of aberrant methylation.

The inflammation induced in the *Helicobacter* groups was characterized by infiltration of mononuclear cells (lymphocytes and macrophages). In our previous study, suppression of T-cell activation by cyclosporin A remarkably repressed inflammatory response and methylation induction triggered by *H.pylori* infection (14), showing that T-cell activation is involved in methylation induction in this system. However, our recent study in mouse colon demonstrated that aberrant methylation can be induced even in severe combined immunodeficiency mice, which lack functional T and B cells, by dextran sulfate sodium-induced colitis (Katsurano *et al.*, submitted for publication). It is known that, even in severe combined immunodeficiency mice, colitis with macrophage infiltration can be induced (36). If a common mechanism for methylation induction is present in *H.pylori*-infected gastric mucosae and dextran sulfate sodium-treated colonic mucosae, infiltration of macrophages is a candidate for the proximate effector that transmits signal for methylation induction to epithelial cells. It can be considered that, in *H.pylori*-infected gastric mucosae, activation of T cells is required only for the initiation or maintenance of inflammation capable of inducing aberrant DNA methylation.

Among the inflammation-related genes, *Il1b*, *Nos2* and *Tnf* were specifically upregulated in the three *Helicobacter* groups. These three genes are reported to be overexpressed also in human chronic inflammation associated with cancers, such as ulcerative colitis and hepatitis (37–40). *IL1B* promoter polymorphism is associated with risk of human gastric cancers (28) and aberrant methylation of multiple genes in gastric cancers (29). The lack of its upregulation in human gastric mucosae infected with *H.pylori* could be because most of them had superficial gastritis and had already increased *IL1B* expression. *NOS2*, which encodes nitric oxide synthase, was upregulated *in vitro* by administration of IL1B and nitric oxide donors induced methylation of *FMR1* and *HPRT* (41). These suggest that IL1B and NOS2 might be involved in methylation induction. On the other hand, *Ifng*, *Il2*, *Il4* and *Il6* were upregulated mainly in the EtOH and NaCl groups, in which no methylation was induced, and also in the SS1 and HF groups, in which methylation induction levels were lower than in the ATCC group. This suggested a possibility that some (one) of the genes could suppress methylation induction.

SS1 and *H.felis*, which lack CagA, were capable of inducing aberrant methylation although the capacity was weaker than the CagA-positive strain (*H.pylori* ATCC 43504). CagA-positive *H.pylori* strains are known to induce severe gastritis in Mongolian gerbils (16) as confirmed in this study, and this explains their stronger capacity to induce methylation. The three inflammation-related genes associated with methylation induction (*Il1b*, *Nos2* and *Tnf*) had the highest expression in the ATCC group among the three *Helicobacter* groups. CagA-positive *H.pylori* seems to promote methylation induction by maximizing expression of such genes and minimizing expression of genes that suppress methylation induction.

Dnmts are the final effectors to methylate DNA, and their overexpression was observed in various human cancers (35). Immunohistochemical analyses here revealed that Dnmt1 was upregulated in gastric mucosae of gerbils in the three *Helicobacter*-infected groups and the NaCl-treated group. However, the highest expression was observed in the NaCl group, where methylation was not induced. This result indicated that expression of Dnmt1 was not associated with methylation induction but with cell proliferation. Expression of Dnmt3a was significantly but slightly decreased in the ATCC group and this also suggested that the expression itself is not involved in aberrant methylation induction. However, due to the lack of an appropriate antibody, we were not able to exclude the possibility that upregulation of Dnmt3b is involved in methylation induction. Therefore, disturbance in the local balance between Dnmts and factors that protect DNA from aberrant methylation, such as the presence of RNA

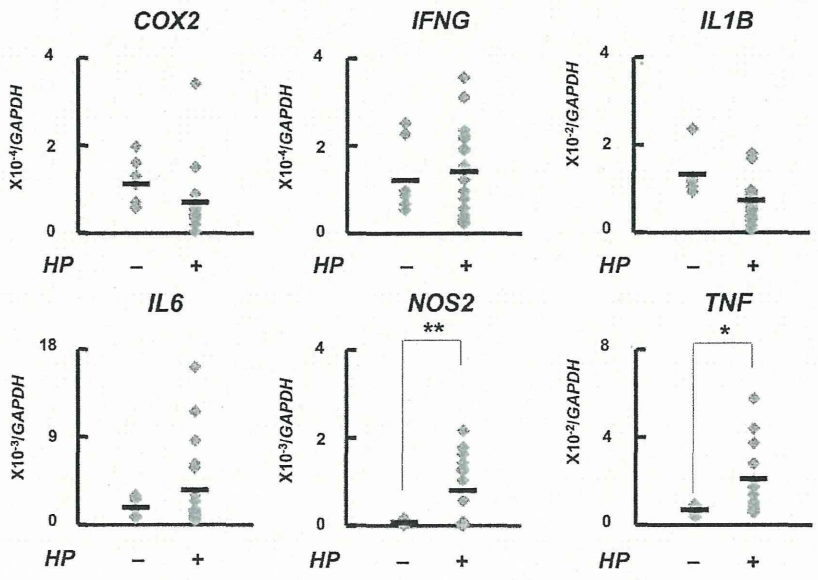

Fig. 5. Human relevance of expression changes in the gerbil stomach. Expression levels of inflammation-related genes were quantified in gastric mucosae of individuals without and with *H.pylori* infection. Bold horizontal bar, the mean expression level; $^{*}P < 0.05$ and $^{**}P < 0.01$.

polymerase II (42) and/or possible overexpression of Dnmt3b might be involved in methylation induction.

In conclusion, inflammation due to infection of *Helicobacter* strains had a high capacity to induce methylation in GECs, regardless of their CagA status. Increased cell proliferation was not sufficient for methylation induction. Therefore, specific types of inflammation, characterized by infiltration of mononuclear cells and expression of specific inflammation-related genes, along with increased cell proliferation were considered to be necessary for methylation induction.

Supplementary material

Supplementary Figures 1–3 and Table 1 can be found at http://carcin.oxfordjournals.org/

Funding

This work was supported by Grants-in-Aid for Cancer Research and for the Third-term Comprehensive Cancer Control Strategy from the Ministry of Health, Labor and Welfare, Japan. K.H. is a recipient of FPCR Fellowship from the Foundation for Promotion of Cancer Research.

Acknowledgements

We thank Dr T.Joh and Dr S.Tajima for their kind provision of a bacterium and antibodies, respectively. We also thank Mr H.Nishikawa (Keyence) for his technical support in microscopic observation.

Conflict of Interest Statement: None declared.

References

1. Jones,P.A. *et al.* (2007) The epigenomics of cancer. *Cell*, **128**, 683–692.
2. Esteller,M. (2008) Epigenetics in cancer. *N. Engl. J. Med.*, **358**, 1148–1159.
3. Issa,J.P. *et al.* (1994) Methylation of the oestrogen receptor CpG island links ageing and neoplasia in human colon. *Nat. Genet.*, **7**, 536–540.
4. Hsieh,C.J. *et al.* (1998) Hypermethylation of the p16INK4a promoter in colectomy specimens of patients with long-standing and extensive ulcerative colitis. *Cancer Res.*, **58**, 3942–3945.
5. Issa,J.P. *et al.* (2001) Accelerated age-related CpG island methylation in ulcerative colitis. *Cancer Res.*, **61**, 3573–3577.
6. Toyota,M. *et al.* (2002) DNA methylation changes in gastrointestinal disease. *J. Gastroenterol.*, **37** (suppl. 14), 97–101.
7. Kondo,Y. *et al.* (2000) Genetic instability and aberrant DNA methylation in chronic hepatitis and cirrhosis—a comprehensive study of loss of heterozygosity and microsatellite instability at 39 loci and DNA hypermethylation on 8 CpG islands in microdissected specimens from patients with hepatocellular carcinoma. *Hepatology*, **32**, 970–979.
8. Maekita,T. *et al.* (2006) High levels of aberrant DNA methylation in Helicobacter pylori-infected gastric mucosae and its possible association with gastric cancer risk. *Clin. Cancer Res.*, **12**, 989–995.
9. Park,S.Y. *et al.* (2009) Comparison of CpG island hypermethylation and repetitive DNA hypomethylation in premalignant stages of gastric cancer, stratified for Helicobacter pylori infection. *J. Pathol.*, **219**, 410–416.
10. Nakajima,T. *et al.* (2006) Higher methylation levels in gastric mucosae significantly correlate with higher risk of gastric cancers. *Cancer Epidemiol. Biomarkers Prev.*, **15**, 2317–2321.
11. Kaise,M. *et al.* (2008) CpG island hypermethylation of tumor-suppressor genes in H. pylori-infected non-neoplastic gastric mucosa is linked with gastric cancer risk. *Helicobacter*, **13**, 35–41.
12. Perri,F. *et al.* (2007) Aberrant DNA methylation in non-neoplastic gastric mucosa of H. Pylori infected patients and effect of eradication. *Am. J. Gastroenterol.*, **102**, 1361–1371.
13. Cotran,R.S. *et al.* (1989) *Robbins Pathologic Basis of Disease*. W.B. Saunders company, Philadelphia, PA.
14. Niwa,T. *et al.* (2010) Inflammatory processes triggered by Helicobacter pylori infection cause aberrant DNA methylation in gastric epithelial cells. *Cancer Res.*, **70**, 1430–1440.
15. Huang,J.Q. *et al.* (2003) Meta-analysis of the relationship between cagA seropositivity and gastric cancer. *Gastroenterology*, **125**, 1636–1644.
16. Shibata,W. *et al.* (2006) CagA protein secreted by the intact type IV secretion system leads to gastric epithelial inflammation in the Mongolian gerbil model. *J. Pathol.*, **210**, 306–314.
17. Crabtree,J.E. *et al.* (2002) The mouse colonizing Helicobacter pylori strain SS1 may lack a functional cag pathogenicity island. *Helicobacter*, **7**, 139–140; author reply, 140–141.
18. De Bock,M. *et al.* (2006) The effect of Helicobacter felis and Helicobacter bizzozeronii on the gastric mucosa in Mongolian gerbils: a sequential pathological study. *J. Comp. Pathol.*, **135**, 226–236.
19. De Bock,M. *et al.* (2006) *Helicobacter felis* and *Helicobacter bizzozeronii* induce gastric parietal cell loss in Mongolian gerbils. *Microbes Infect.*, **8**, 503–510.
20. Kang,J.Y. *et al.* (1995) Effect of capsaicin and chilli on ethanol induced gastric mucosal injury in the rat. *Gut*, **36**, 664–669.
21. Suzuki,H. *et al.* (1999) Ethanol intake preceding Helicobacter pylori inoculation promotes gastric mucosal inflammation in Mongolian gerbils. *J. Gastroenterol. Hepatol.*, **14**, 1062–1069.
22. Furihata,C. *et al.* (1996) Cause and effect between concentration-dependent tissue damage and temporary cell proliferation in rat stomach mucosa by NaCl, a stomach tumor promoter. *Carcinogenesis*, **17**, 401–406.
23. Tatematsu,M. *et al.* (1998) Induction of glandular stomach cancers in Helicobacter pylori-sensitive Mongolian gerbils treated with N-methyl-N-nitrosourea and N-methyl-N'-nitro-N-nitrosoguanidine in drinking water. *Jpn. J. Cancer Res.*, **89**, 97–104.
24. D'Elios,M.M. *et al.* (1997) T helper 1 effector cells specific for Helicobacter pylori in the gastric antrum of patients with peptic ulcer disease. *J. Immunol.*, **158**, 962–967.
25. Fu,S. *et al.* (1999) Increased expression and cellular localization of inducible nitric oxide synthase and cyclooxygenase 2 in Helicobacter pylori gastritis. *Gastroenterology*, **116**, 1319–1329.
26. Yamaoka,Y. *et al.* (2005) Natural history of gastric mucosal cytokine expression in Helicobacter pylori gastritis in Mongolian gerbils. *Infect. Immun.*, **73**, 2205–2212.
27. Toyoda,T. *et al.* (2008) Synergistic upregulation of inducible nitric oxide synthase and cyclooxygenase-2 in gastric mucosa of Mongolian gerbils by a high-salt diet and Helicobacter pylori infection. *Histol. Histopathol.*, **23**, 593–599.
28. El-Omar,E.M. *et al.* (2000) Interleukin-1 polymorphisms associated with increased risk of gastric cancer. *Nature*, **404**, 398–402.
29. Chan,A.O. *et al.* (2007) Association between Helicobacter pylori infection and interleukin 1beta polymorphism predispose to CpG island methylation in gastric cancer. *Gut*, **56**, 595–597.
30. Lee,A. *et al.* (1997) A standardized mouse model of Helicobacter pylori infection: introducing the Sydney strain. *Gastroenterology*, **112**, 1386–1397.
31. Cheng,H. *et al.* (1984) Methods for the determination of epithelial cell kinetic parameters of human colonic epithelium isolated from surgical and biopsy specimens. *Gastroenterology*, **86**, 78–85.
32. Toyoda,T. *et al.* (2007) Inhibitory effect of nordihydroguaiaretic acid, a plant lignan, on *Helicobacter pylori*-associated gastric carcinogenesis in Mongolian gerbils. *Cancer Sci.*, **98**, 1689–1695.
33. Takagi,H. *et al.* (1995) Overexpression of DNA methyltransferase in myoblast cells accelerates myotube formation. *Eur. J. Biochem.*, **231**, 282–291.
34. Aoki,A. *et al.* (2001) Enzymatic properties of de novo-type mouse DNA (cytosine-5) methyltransferases. *Nucleic Acids Res.*, **29**, 3506–3512.
35. Kanai,Y. *et al.* (2007) Alterations of DNA methylation associated with abnormalities of DNA methyltransferases in human cancers during transition from a precancerous to a malignant state. *Carcinogenesis*, **28**, 2434–2442.
36. Dieleman,L.A. *et al.* (1994) Dextran sulfate sodium-induced colitis occurs in severe combined immunodeficient mice. *Gastroenterology*, **107**, 1643–1652.
37. Cappello,M. *et al.* (1992) Detection of mRNAs for macrophage products in inflammatory bowel disease by in situ hybridisation. *Gut*, **33**, 1214–1219.
38. McLaughlan,J.M. *et al.* (1997) Interleukin-8 and inducible nitric oxide synthase mRNA levels in inflammatory bowel disease at first presentation. *J. Pathol.*, **181**, 87–92.
39. Llorente,L. *et al.* (1996) Cytokine gene expression in cirrhotic and non-cirrhotic human liver. *J. Hepatol.*, **24**, 555–563.
40. Mihm,S. *et al.* (1997) Hepatic expression of inducible nitric oxide synthase transcripts in chronic hepatitis C virus infection: relation to hepatic viral load and liver injury. *Hepatology*, **26**, 451–458.
41. Hmadcha,A. *et al.* (1999) Methylation-dependent gene silencing induced by interleukin 1beta via nitric oxide production. *J. Exp. Med.*, **190**, 1595–1604.
42. Takeshima,H. *et al.* (2009) The presence of RNA polymerase II, active or stalled, predicts epigenetic fate of promoter CpG islands. *Genome Res.*, **19**, 1974–1982.

Received May 11, 2010; revised September 29, 2010; accepted October 19, 2010

Ann Surg Oncol (2011) 18:1185–1194
DOI 10.1245/s10434-010-1393-5

Annals of
SURGICAL ONCOLOGY
OFFICIAL JOURNAL OF THE SOCIETY OF SURGICAL ONCOLOGY

ORIGINAL ARTICLE – TRANSLATIONAL RESEARCH AND BIOMARKERS

Identification and Validation of DNA Methylation Markers to Predict Lymph Node Metastasis of Esophageal Squamous Cell Carcinomas

Ken Gyobu, MD[1,2], Satoshi Yamashita, PhD[1], Yasunori Matsuda, MD[1,2], Hiroyasu Igaki, MD, PhD[3], Tohru Niwa, PhD[1], Daiji Oka, MD[1], Ryoji Kushima, MD, PhD[4], Harushi Osugi, MD, PhD[2], Shigeru Lee, MD[2], Shigefumi Suehiro, MD, PhD[5], and Toshikazu Ushijima, MD, PhD[1]

[1]Carcinogenesis Division, National Cancer Center Research Institute, Tokyo, Japan; [2]Department of Gastrointestinal Surgery, Graduate School of Medicine, Osaka City University, Osaka, Japan; [3]Esophageal Surgery Division, National Cancer Center Hospital, Tokyo, Japan; [4]Pathology of Clinical Laboratory Division, National Cancer Center Hospital, Tokyo, Japan; [5]Department of Cardiovascular Surgery, Graduate School of Medicine, Osaka City University, Osaka, Japan

ABSTRACT

Background. The presence of lymph node metastasis in esophageal squamous cell carcinoma (ESCC) patients is a critical factor for decision of treatment strategy. However, there have been no molecular markers to assess lymph node metastasis. In this study, we aimed to identify CpG islands (CGIs) whose DNA methylation statuses are associated with the presence of lymph node metastasis.

Materials and Methods. A total of 96 ESCCs were divided into a screening set ($n = 48$) and a validation set ($n = 48$). Genome-wide methylation analysis was performed by methylated DNA immunoprecipitation-CGI microarray analysis. Methylation levels were analyzed by quantitative methylation-specific PCR (qMSP).

Results. Genome-wide methylation analysis identified 25 CGIs differentially methylated between 8 ESCCs with lymph node metastasis and 4 without. In the screening set, 7 CGIs had significantly different methylation levels ($P < 0.05$) between the ESCCs with and without lymph node metastasis, and cut-off methylation levels for these CGIs were determined. The validation set was analyzed with the prefixed cut-offs, and methylation statuses of 2 CGIs in the vicinities of *PAX6* and ENST00000363328 were validated to be associated with the presence of lymph node metastasis. Using these 2 markers, the presence was predicted with a sensitivity of 93% and specificity of 57%. In addition, the methylation statuses of the 2 CGIs were significantly associated with disease-free survival ($P = 0.006$).

Conclusions. Methylation statuses of these 2 CGIs were significantly associated with the presence of lymph node metastasis of ESCCs. These CGIs are promising markers to predict the presence of lymph node metastases.

First Received: 19 April 2010;
Published Online: 2 November 2010

T. Ushijima, MD, PhD
e-mail: tushijim@ncc.go.jp

Esophageal squamous cell carcinoma (ESCC) is still one of the most lethal cancers in spite of recent advancements in its diagnostics and therapeutics. One of the reasons for its poor prognosis is the fact that ESCCs frequently metastasize to regional and distant lymph nodes at early stages.[1] To avoid risk of recurrence from metastatic lymph nodes, esophageal resection with extended lymph node dissection has been performed as a standard therapy, even though this surgery has high morbidity and mortality.[2,3] If the presence of lymph node metastasis can be predicted accurately before operation, we can avoid unnecessary lymph node dissection, which can decrease morbidity and mortality at operations, and open a new avenue for ESCC treatment strategies.

To predict the presence of lymph node metastasis accurately before operation, much effort has been made in the fields of imaging and molecular markers. Imaging, such as computed tomography (CT), endoscopic ultrasonography (EUS), and fluorine ^{18}F-fluorodeoxyglucose positron emission tomography (FDG-PET), is used in clinical practice. However, these procedures have only limited ability to detect small metastatic lymph nodes, with a

reported sensitivity of 31%–48%, 85%, and 51%–64%, respectively, and specificity of 79%–86%, 85%, and 69%–90%, respectively, and are almost powerless to detect micrometastasis.[4–7] Regarding molecular markers, few studies on protein or mRNA expression to predict lymph node metastasis have been validated. Therefore, a marker with a high accuracy is awaited.

Aberrant DNA methylation is deeply involved in the development and progression of human cancers and is expected to provide useful cancer pathophysiology markers for several reasons.[8–10] First, the DNA methylation status is stable regardless of cellular environment and thus can predict that a gene, such as *MGMT*, will never be expressed in the future.[11,12] Secondly, DNA methylation has only 2 statuses, methylated or unmethylated, while gene expression has a large range of variation. Therefore, an overall DNA methylation profile in a heterogeneous sample is not blurred by the methylation status of a minor population of cells, while an overall gene expression profile can be strongly influenced by that of a minor population of cells. Thirdly, DNA methylation can be assessed using DNA, which is chemically more stable than RNA and proteins, and has advantages in clinical applications.[10] Taking these advantages, excellent DNA methylation markers have already been identified and validated in some cancers.[13,14] In ESCCs, methylation statuses of some genes are reported to be associated with lymph node metastasis, such as *RARβ* ($P = 0.046$), *hMLH1* ($P < 0.0001$), *PLCd1* ($P = 0.014$), *ECRG4* ($P = 0.009$), and *UCHL1* ($P = 0.03$).[15–19] These associations are waiting to be validated, and their sensitivity and specificity need to be established.

In the present study, we aimed to identify CpG islands (CGIs) whose methylation statuses are associated with the presence of lymph node metastasis of ESCCs by a genome-wide methylation analysis and to validate their usefulness.

MATERIALS AND METHODS

Patients, Tissue Samples, and DNA Extraction

A total of 96 ESCC samples (average age, 64 years [range, 41–82 years]; 79 male and 17 female), along with 3 metastatic lymph nodes, were obtained from patients who underwent esophagectomy with extended lymph node dissection at the National Cancer Center Hospital and Osaka City Medical University Hospital from 2006 to 2008 with informed consent. No patients had undergone prior chemotherapy or radiotherapy. Curative resection (R0), esophagectomy with 2- or 3-field lymphadenectomy, was performed in 91 patients, and noncurative resection (R2) was performed in the remaining 5 patients, who were excluded from the survival analysis. The mean follow-up period after operation was 27.4 months. None of the patients died of postoperative complications. Disease grades were classified according to the 6th edition of the TNM classification by the UICC.[20] Imaging data was available for 67 patients, and metastasis to lymph nodes was considered to be positive if a lesion larger than 5 mm in the short axis was present on CT or EUS, or a lesion revealed internal hypoechogenicity and a rounded shape on EUS, or a lesion showed focally abnormal FDG uptake on EDG-PET. Samples were stored at −80°C, and high molecular weight DNA was extracted by the phenol/chloroform method. The 96 cancer samples were randomly divided into screening ($n = 48$) and validation ($n = 48$) sets, which contained 7 and 8 N0 samples, respectively.

Cell Lines

The ESCC cell lines KYSE30, KYSE50, KYSE220, and KYSE270 were purchased from Health Science Research Resources Bank (Osaka, Japan).[21] Total RNA was extracted using Isogen (Nippon Gene, Tokyo, Japan).

Genome-Wide Methylation Analysis by Methylated DNA Immunoprecipitation (MeDIP)-CGI Microarray

Two kinds of genome-wide screening were performed (1) comparison between primary ESCCs with and without lymph node metastasis and (2) comparison between primary ESCCs without lymph node metastasis and metastatic lymph nodes. If a DNA methylation alteration associated with lymph node metastasis occurs in a small fraction of cells in primary ESCCs, a methylation level in the primary ESCCs is expected to be too low to be detected by genome-wide screening. However, in metastatic lymph nodes, all cancer cells are expected to carry the methylation alteration, and methylation levels in the lymph nodes are expected to be high enough to be identified by genome-wide screening.

MeDIP-CGI microarray analysis was performed as previously described.[22,23] Briefly, 5 μg of genomic DNA was immunoprecipitated with an anti-5-methylcytidine antibody (Diagnode, Liége, Belgium), and the precipitated DNA and the input DNA were labeled with Cy5 and Cy3, respectively. A human CGI oligonucleotide microarray (Agilent technologies, Santa Clara, CA) was hybridized with the labeled probes and scanned with an Agilent G2565BA microarray scanner (Agilent Technologies). Scanned data were processed with Feature Extraction Ver.9.1 and Agilent G4477AA ChIP Analytics 1.3 software. A signal of a probe was converted into a "Me value," which represented the methylation level as a value from 0 (unmethylated) to 1 (methylated).[22] Differentially methylated regions were detected by comparison of the Me values of the 2 samples. When 3 or more consecutive probes in a

locus showed differences in the Me value larger than 0.4, the locus was considered to have different methylation statuses (representative loci are shown in Fig. 1). The microarray results were submitted to the GEO database (GSE21238).

Semiquantitative Methylation-Specific PCR (Semi-qMSP) and Quantitative MSP (qMSP)

A fully methylated control was prepared by methylating genomic DNA with *Sss*I methylase (New England Biolabs, Beverly, MA). One μg of DNA digested with *Bam*HI was treated with sodium bisulfite and suspended in 40 μL of TE buffer as described.[24] An aliquot of 2 μL was used as a template for semi-qMSP and qMSP. Semi-qMSP and qMSP were performed by real-time PCR using primers specific to DNA molecules methylated at a target locus and to a methylated *Alu* repeat sequence (Table 1).[25] In semi-qMSP, differences of methylation levels were assessed as differences of relative Ct values [Ct (target locus) – Ct (*Alu* repeat sequence)], and differences ≥2 were considered significant. In qMSP, as methylation levels, a percentage of the methylated reference was calculated as {(No. of fragments methylated at a target locus in a sample)/(No. of *Alu* repeat sequences in the sample)}/{(No. of fragments methylated at a target locus in *Sss*I-treated DNA)/(No. of *Alu* repeat sequences in the *Sss*I-treated DNA)} × 100.[26,27]

Quantitative Reverse Transcription-PCR (qRT-PCR)

qRT-PCR was performed by real-time PCR as previously described, and the mRNA quantity of a gene was normalized to that of *B2M* (beta-2-microglobulin).[28] *PAX6* cDNA was amplified with a forward primer (5′-TGGA GAAAGAGTTTGAGAGA-3′) and a reverse primer (5′-AACCATACCTGTATTCTTGC-3′). *B2M* cDNA was amplified with a forward primer (5′-TGCTGTCTCCATG TTTGATGTATCT-3′) and a reverse primer (5′-TCTCTG CTCCCCACCTCTAAGT-3′).

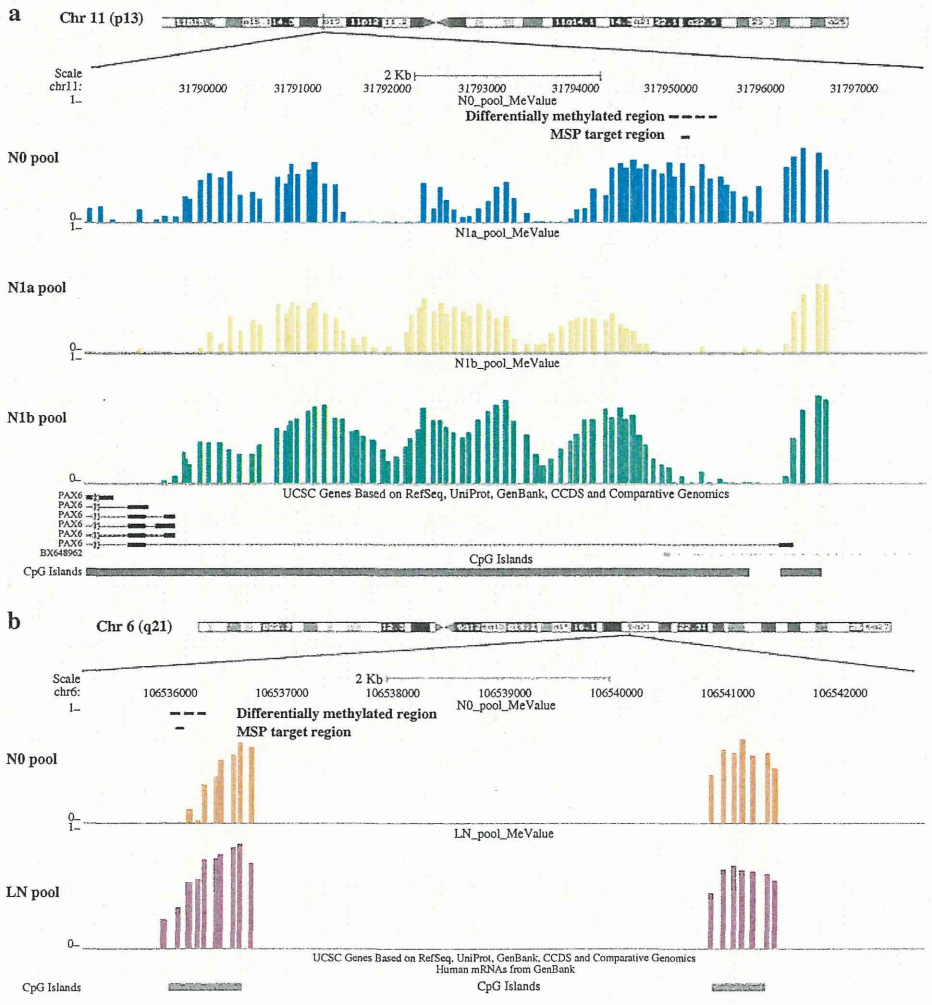

FIG. 1 Data of MeDIP-CGI microarray analysis in genomic regions around CGI No. 5 (**a**) and No. 21 (**b**). Methylation levels were assessed by Me values, and the Me values in this region are shown for the pools of samples. Vertical bars show Me values of each probes. Dashed lines show the areas where differences in Me values were larger than 0.4 between the N0 and two N1 pools (**a**) or between the N0 and LN pools (**b**). MSP primers were designed in the area shown by a black line. This figure was drawn by the UCSC Genome Browser (http://genome.ucsc.edu/) on NCBI36/hg18 assembly that shows the nucleotides from 31,788,500 to 31,797,500 on chromosome 11 (**a**) and from 106,535,000 to 106,542,500 on chromosome 6 (**b**)

TABLE 1 CGIs identified by methylation-microarray analysis and semi-qMSP

No.	Gene symbol	Location		AT	dCt	Cut-off (%)	AUC	*P* value*		Primer sequence for MSP		ANT
		Chr	nt. number					Scr	Val	Forward	Reverse	
CGIs identified by comparison between the N0 pool and N1 pools (hypermethylated in the N0 pool)												
1	CA8	8	061355936–061356740	P–I	–5.9	0.6	0.62	0.050	0.214	TAGTGTTTCGTCGAGCGC	AACGCAAACGACGAACACG	62
2	CPLX2	5	175156233–175156526	I	–2.1	2	0.77	0.006	0.183	TTGGCGTTTTTCGCGTGTAC	AAACGAACGCGCGTTCTACG	63
3	ENST00000355099	8	144924874–144925131	U	–2.2	64	0.5	0.116	–	GGTATTCGCGTGGTTCGATAGTTTC	CAATAAAACGCTTATAACGCTTCCG	65
4	HOXA10	7	027180516–027180721	P	–2.2	0.3	0.77	0.020	1.000	TAATCGCGGGTTTTGAGGGC	CCCGAACCAAAATTTCCGCG	65
5	PAX6	11	031794729–031795212	P	–4.1	2	0.79	0.048	0.033	GGATTTTCGTTCGATTTCGAGC	ACCCAAATAAAACGTACGACCG	55
CGIs identified by comparison between the N0 pool and N1 pools (hypomethylated in the N0 pool)												
6	CEI	5	002809698–002809918	D	3	8.7	0.59	0.174		ATGAAATGTTTGAAATTTCGTCGTC	AACTTCAACGAAACGCGCCG	66
7	EBF2	8	025958035–025958319	I	4.3	3.2	0.61	0.116	–	TTGGGCGCGGAGATGGATTC	ACATAATAATTACGCGACCGTATCG	68
8	ENST00000362901	16	049432503–049432929	U	2.4	10	0.64	0.064	–	GCGGTTGTTTTTGTATGCGTCGC	CGCCTCGCCTCCTATCTCGATAACG	69
9	FOXB2	9	078821358–078821553	P	3	16	0.59	0.229	–	GGAGTCGTAAGTGTTTAACGGGTAC	CCGAACTTCGACCCCACACG	65
10	FOXL2	3	140146707–140146878	I	5.6	0.9	0.58	0.115	–	TGCGATCGGGCGTCGGTAGC	CTACACGACAATCGAACGAAAAACG	62
11	GNG3	11	062233548–062233783	D	3.8	12.9	0.48	0.659		GTTTTAATTAAGTCGGGGTTCGC	TAATTCTTCGTTATAACCGCCCG	64
12	hsa-let-7i	12	061311792–061312529	U	3.3	18	0.52	0.123	–	AGAGGTTGCGGGTTAGGCGGTC	ACCGTAACCCAAACTCCCCGCG	67
13	hsa-mir-137	1	098291535–098291818	P	4.4	8.5	0.76	0.014	0.662	TAGAGTGATTTCGGCGTTCGC	TTACGCTCTTCACTTCGCCAAACG	70
14	MEIS1	2	066506991–066507361	P	3.6	28	0.54	0.170	–	ATAGAAGTCGGTGCGTTATCGTC	CGATAAATAACAACCCGAAAACCG	65
15	NBEA	13	034942753–034942962	I	5	3.8	0.62	0.055	–	GGAGCGGTTCGAATCGGTTC	TATACGCGCGCTTAACGACG	68
16	RARG	12	051899907–051900229	I	4.1	12	0.57	0.437	–	TAAGTCGGGTCGCGATGTAC	AAACCGCCGATAACTCTACG	65
17	TBX4	17	056894148–056894368	I	4.9	16	0.5	0.230	–	GTTTTTAATATCGAGAAACGTTC	ATAAACAAACCGCCTACTCG	55
18	WT1	11	032411811–32412319	I	3.2	20	0.69	0.228	–	CGTCGTGTTCGTGGATAGTTTTCGC	ACGTAACCGCCGCCTAAACG	65
CGIs identified by comparison between the LN pool and N0 pool (hypermethylated in the N0 pool)												
19	EGFR	7	055053568–055053786	P	–2.2	8	0.7	0.018	1.000	GACGTTTGGTATTTTTGTCGCGC	CCAACGTCGAATAATAACACCGACG	65
20	STAT5A	17	037718039–037718317	D	–2.9	3.9	0.53	0.407	–	TTAGTAGGTGGTATTACGCGGTTGC	ACCGAAACGAACCGATCCCG	65
CGIs identified by comparison between the LN pool and N0 pool (hypomethylated in the N0 pool)												
21	ENST00000363328	6	106535908–106536096	U	6.9	8.3	0.69	0.045	0.044	ATGGAATAGTTTAGTCGGTGAGTTC	ATATTCCCAAACGAATACGAACG	63
22	FLJ32569	1	204085584–204085901	P–I	2.6	1.3	0.61	0.236	–	TGGTTTAGCGGTGCGTTTGC	CTAAACTAAAAAAAAATTCGCGACG	68
23	PDGFRA	4	054791871–054792165	I	3.4	1	0.54	0.088	–	TTTGGTTTCGCGTTTTGGTC	AACGAAATACGAAACCGACG	65
24	PLEKHA7	11	016991355–016991625	I	2.4	4.8	0.47	0.240	–	TTTTCGGTCGGAGTTGAATC	ACTAATACGCCAACACTCCG	65
25	TMEM97	17	023669398–023669584	P	3	0.2	0.64	0.064	–	GTAGTTTCGGCGATTTTGTTTC	AAATCAAAAATTCGTTTACACG	62

Chr chromosome number, *nt. number* nucleotide number in the NCBI data base (NCBI36/hg18), *AT* annotation type, *U* upstream, *P* promoter, *I* inside, *D* downstream, *dCt* difference of mean Ct value in semi-qMSP, *cut-off* cut-off methylation level determined by ROC curve, *AUC* area under the ROC curve, *Scr* screening set, *Val* validation set, *ANT* annealing temperature for real-time MSP (°C)

* Statistically significant values: $P < 0.05$

Statistical Analyses

Differences in methylation incidences between ESCCs with and without lymph node metastasis and associations between methylation status and various clinicopathological parameters were evaluated by Fisher exact test (2-sided). The confounders affecting the apparent likelihood of the presence of lymph node metastasis were tested using multivariate logistic regression analysis. Disease-free survival was calculated from the date of operation to that of relapse. Survival curves were computed according to the Kaplan–Meier method and were compared by the log-rank test. All statistical analyses were conducted by PASW statistics version 18.0.0 (SPSS Japan Inc., Tokyo, Japan).

RESULTS

Isolation of CGIs Whose Methylation Statuses were Associated with the Presence of Lymph Node Metastasis

A pool of 4 cancer samples without lymph node metastasis (N0 pool), 2 pools of 4 cancer samples with lymph node metastasis (N1a and N1b pools), and 1 pool of 3 metastatic lymph nodes (LN pool) were prepared from the patients in the screening set, and analyzed by MeDIP-CGI microarray. By comparisons between the N0 and N1a pools and between N0 and N1b pools, 11 and 26 CGIs were identified as hypermethylated and hypomethylated, respectively, in the N0 pool (a representative locus in Fig. a). By comparison between the LN and N0 pools, 5 and 12 CGIs were identified as hypermethylated and hypomethylated, respectively, in the N0 pool (a representative locus in Fig. b). A total of 52 CGIs were isolated because 2 of the 54 (11 + 26 + 5 + 12) CGIs were duplicately isolated in the 2 kinds of screenings.

To confirm the results of MeDIP-CGI microarray analysis, methylation levels of these CGIs were then evaluated by semi-qMSP in the 12 primary cancer samples used for the N0, N1a, and N1b pools. Because primers for semi-qMSP could not be designed for 2 CGIs, the remaining 50 CGIs were analyzed. Hypermethylation and hypomethylation in the N0 pool were confirmed for seven and 18 CGIs, respectively (Table).

Selection of CGIs Whose Methylation was Associated with Lymph Node Metastasis in the Screening Set

Methylation levels of the 25 CGIs were quantified in the screening set by qMSP, and receiver operating characteristic (ROC) curves for detection of ESCCs with lymph node metastasis were constructed. For each CGI, a cut-off methylation level was determined so that the vertical distance between the ROC curve and diagonal line (Youden index = sensitively + specificity − 1) would be maximized. Significant association between methylation status and the presence of lymph node metastasis was observed for 7 CGIs. Also, 5 CGIs (No. 1, 2, 4, 5, and 19 in Table) were hypermethylated in ESCCs without lymph node metastasis, and 2 CGIs (No. 13 and 21 in Table) were hypomethylated in ESCCs without lymph node metastasis.

Validation of the Selected CGIs in the Validation Set

To validate the association observed for the 7 CGIs in the screening set, their methylation levels were quantified in the same manner, and association with the presence of lymph node metastasis was analyzed with the prefixed cut-off methylation levels in the validation set. Hypermethylation of CGI No. 5 and hypomethylation of CGI No. 21 in ESCCs without lymph node metastasis were validated, showing that the unmethylated status of CGI No. 5 and methylated status of CGI No. 21 can predict the presence of lymph node metastasis (Fig.). The sensitivity, specificity, and accuracy of CGI No. 5 were 73%, 71%, and 73%, respectively. Those of CGI No. 21 were 59%, 86%, and 63%, respectively. A cancer sample was regarded as positive for lymph node metastasis if at least 1 of CGI No. 5 and No. 21 was positive, those being 93%, 57%, and 85%, respectively.

Comparison between Methylation Markers and Conventional Imaging

To compare the sensitivity and specificity of the methylation markers with those of conventional imaging, we assessed the sensitivity and specificity of CT, EUS, and their combination along with FDG-PET in the patients in this study (both the screening and validation sets). The sensitivity and specificity to detect the presence of lymph node metastasis were 88 and 7%, respectively, for CT ($n = 65$), and 88 and 11%, respectively, for EUS ($n = 49$). The sensitivity and specificity of a combination of conventional imaging were 91 and 0%, respectively ($n = 67$), while those of methylation markers (a combination of CGIs No. 5 and No. 21) were 93 and 57%, respectively.

Expression Analysis of PAX6

CGI No. 5 was located 5300 bp upstream from the transcriptional start site (TSS) of most variants of *PAX6* and 1,200 bp downstream from the TSS of one variant (Fig.). Although methylation of CGI No. 5 was unlikely to be associated with repression of *PAX6* expression, it was quantified in four ESCC cell lines by qRT-PCR. *PAX6* was expressed in 3 cell lines (KYSE50, KYSE220, and KYSE270) with methylation of CGI No. 5 (data not

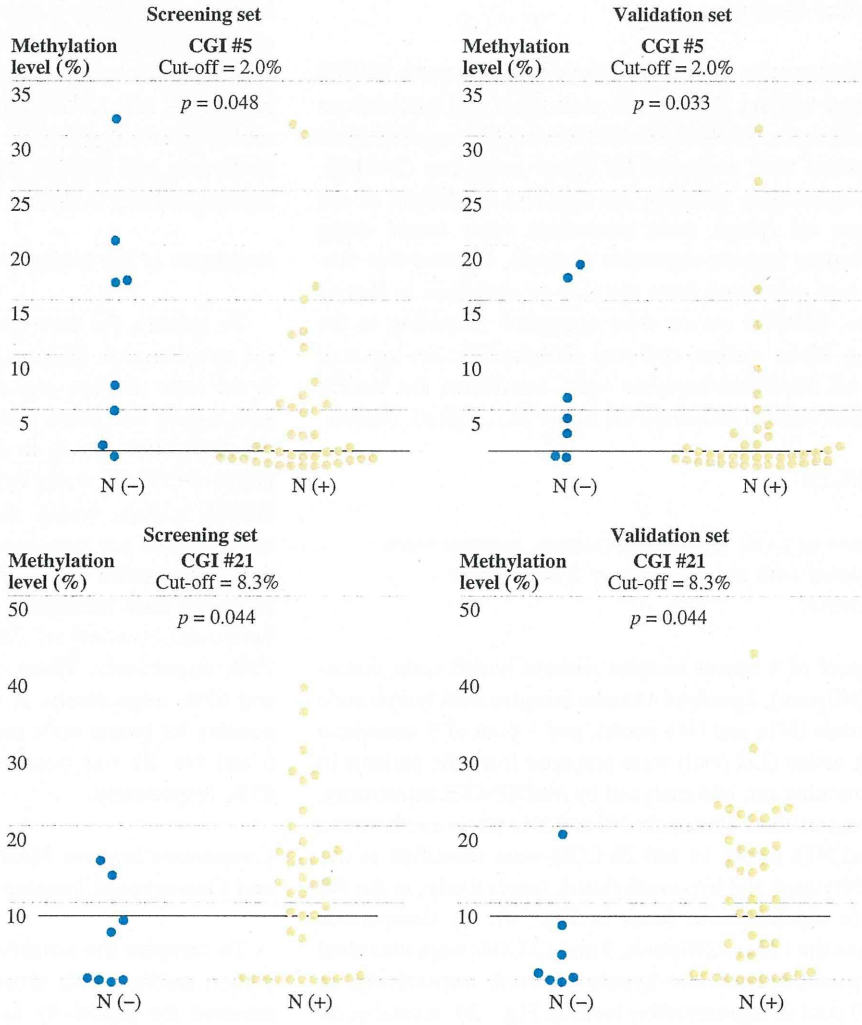

FIG. 2 Distribution of methylation levels of CGIs No. 5 and No. 21 in the screening (*left*) and validation (*right*) sets. N(−), ESCCs without lymph node metastasis; N(+), those with lymph node metastasis. Horizontal lines represent the cut-off methylation levels, which were obtained in the screening set and prefixed in the validation set. Unmethylated CGI No. 5 and methylated CGI No. 21 were associated with the presence of lymph node metastasis

shown), and repression of *PAX6* expression by methylation of CGI No. 5 CGI was ruled out. Regarding CGI No. 21, it was located 80,000 bp away from ENST00000363328, and expression analysis was not performed.

Association with Clinicopathological Characteristics

Univariate analyses were conducted for associations between methylation statuses of CGIs No. 5 and No. 21 and clinicopathological characteristics (histological differentiation, T category, lymphatic invasion, vascular invasion, and lymph node metastasis) (Table 2). The methylation status of CGI No. 5 was associated only with lymph node metastasis, and that of CGI No. 21 was associated also with lymphatic invasion. Multivariate analysis was therefore conducted after exclusion of lymphatic invasion. The presence of lymph node metastasis was shown to be influenced by methylation statuses of CGI No. 5 and No. 21 independently of T category, vascular invasion, age, and gender (Table 3).

By Kaplan–Meier analysis, patients with unmethylated CGI No. 5 had significantly worse disease-free survival than those with methylated CGI No. 5 ($P = 0.014$; Fig. 3a). The methylation status of CGI No. 21 was not significantly associated with disease-free survival ($P = 0.24$). However, a combination of CGIs No. 5 and No. 21 in the prediction of the lymph node metastasis showed more significant association with disease-free survival ($P = 0.006$). When patients were stratified by their T category, which is known to be associated with disease-free survival, significant association was observed within the T3 subgroup, and similar trends were observed within the T2 subgroup (Fig. 3b). T1 and T4 subgroups were not analyzed because they contained small number of patients (1 relapse of 7 patients in the T1 subgroup, and 3 relapses of 3 patients in the T4 subgroup).